Equivalent circuit models of finite slot antennas

van Schelven, Ralph; Cavallo, Daniele; Neto, Andrea

Publication date
2019

Document Version
Accepted author manuscript

Published in
2019 13th European Conference on Antennas and Propagation (EuCAP)

Equivalent Circuit Models of Finite Slot Antennas

Ralph M. van Schelven[1], Daniele Cavallo[1], and Andrea Neto[1]
[1]Terahertz Sensing Group, Microelectronics dept., Delft University of Technology, Delft, The Netherlands,
r.m.vanschelven@tudelft.nl

***Abstract*—We propose a systematic approach to describe planar slot antennas, embedded in generic stratified media. An equivalent transmission line model for the slot is proposed, based on a spectral domain analysis. First, we introduce a method of moments solution to model semi-infinite or finite slots, fed by a delta-gap excitation. The solution entails only two basis functions, one located at the feed and the other at the terminations. The latter basis function is chosen to properly account for the field diffractive behavior at the antenna end points. An approximate circuit model is then introduced, which describes the main mode propagating along the slot as an equivalent transmission line. Lumped impedances are extracted to accurately describe the source and the end points: the reactances account for the reactive nature of the feed and the termination, while the resistances represent the radiated space waves, emerging from both the feed and the end points. This procedure can be used to derive the input impedance of planar antennas with arbitrary length in generic layered media or the interaction between multiple feeds within the same slot.**

***Index Terms*—Equivalent circuit, input impedance, slot antenna.**

I. Introduction

Printed slot antennas are among the most common planar antennas in use today and have been studied extensively in the literature, both as isolated elements and in array configurations. Their structure is complementary to the printed dipoles, thus all known analytical solutions of canonical dipole antennas can be applied also to slots by using Babinet's principle [1]. However, realistic slot antennas are not radiating in free space but in the presence of a more complex dielectric stratification. In these cases, the input impedance is typically determined with general-purpose numerical methods.

A convenient way to describe a center-fed slot is by an equivalent transmission line model, where the excitation is modeled as a shunt generator and the slot arms are represented as two transmission line sections. For example, equivalent transmission line models were used in [2]–[4] to aid the design of slot antennas with different loadings. To compute the characteristic impedance and the propagation constant of the slot lines, different methods have been proposed in [5]–[7]. Transmission line models for slot antennas were given in [8], [9]. In particular, the approach in [8] was based on equating the power radiated by the slot to the power delivered to a lossy transmission line. However, both the equivalent transmission lines considered short circuits to describe the slot terminations, thus did not account for the reactance associated with the end points. An improved model was proposed in [10], where the inductance of the slot shorted ends was considered.

However, all the existing models do not account for the reactance of the feed and the diffraction from the edge. Moreover the radiation is modeled as a distributed resistance through a lossy line or as a single lumped resistance. A different approach is presented here, where an improved model is proposed that accurately describes the reactive nature of both the feed and the terminations of the slot. First, a Method of Moments (MoM) solution is given where, by using the Green's function of an infinite slot [11], only two basis functions are employed to describe the current in the feeding gap and at the edges of the antennas. The basis functions are appropriately chosen to represent the reactance due to finite dimension of the feed and due to the diffraction of the electromagnetic field at the end points. Moreover, the MoM solution allows representing the radiation from the slot in terms of three separate resistances, one associated with the feed point and two located at the edges. Such configuration give more physical insight, as the radiated field can be interpreted as three space waves, emerging from the feed and the end points.

An additional advantage of the proposed method is that the characteristic impedance of the transmission line is derived by extracting the polar singularity contribution of the spectral domain Green's function as in [12], [13], thus can be generalized to arbitrary stratified media, as long as the polar and the branch singularity do not coincide.

II. MoM Solution for Semi-Infinite Slot

This section describes an efficient MoM calculation to compute the input impedance and the magnetic current distribution of a semi-infinite slot in stratified media. The x-oriented slot is assumed to be electrically narrow and excited by a feeding gap, which is small in terms of the wavelength (δ-gap excitation). First, an infinite slot is considered as in [12], where it was shown that the voltage along the slot is represented accurately by:

$$v(x) = \frac{1}{2\pi}\int_{-\infty}^{\infty} \frac{i_\delta F_\delta(k_x)}{D_s(k_x)} e^{-jk_x x} dk_x \tag{1}$$

where i_δ is the average current in the feeding gap, $F_\delta(k_x)$ is the spectral basis function representing the magnetic field excited in the gap:

$$F_\delta(k_x) = \text{sinc}\left(\frac{k_x \delta}{2}\right) \tag{2}$$

and

$$D_s(k_x) = \frac{1}{2\pi}\int_{-\infty}^{\infty} G_{xx}^{hm}(k_x, k_y) M_t(k_y) dk_y \tag{3}$$

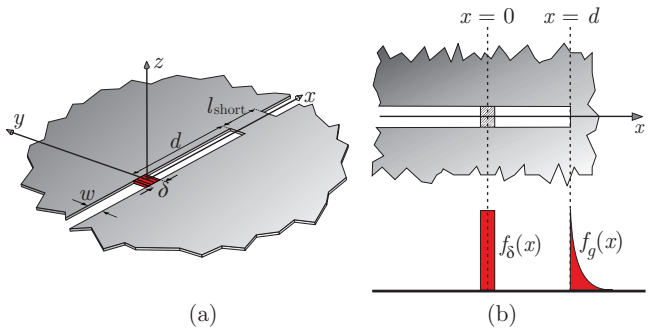

Fig. 1. (a) Interrupted infinite slot in free space. (b) Space domain basis functions with respect to their location along the semi-infinite slot.

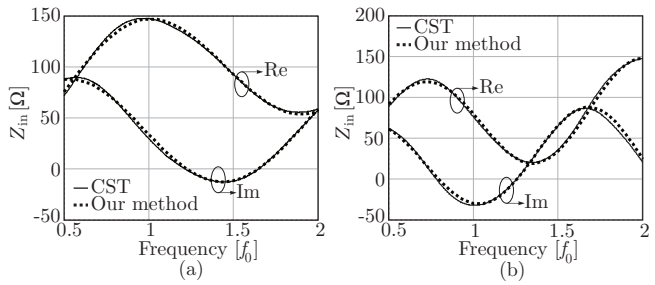

Fig. 2. Comparison between the input impedance of a semi-infinite slot calculated with our method and CST. The geometrical parameters of the structure are $d = \lambda_0/4$, $w = \lambda_0/50$ and $\delta = \lambda_0/40$. λ_0 is the wavelength in free space at f_0. (a) The slot is surrounded by free space. (b) A thin dielectric substrate is added: $\varepsilon_r = 4$, $h = \lambda_d/20$ when λ_d is the wavelength in the dielectric at f_0.

is the spectral longitudinal Green's function of an infinite slot. G_{xx}^{hm} is the xx-component of the spectral dyadic Green's function relating magnetic field to magnetic source, and k_x and k_y are the spectral counterparts of the spatial variables x and y, respectively. As the transverse current distribution is assumed to be edge-singular, its Fourier transform is $M_t(k_y) = -J_0\left(k_y w/2\right)$. The integral in (3) can be solved analytically for free space, while it is computed numerically for generic stratification.

We now interrupt the infinite slot with a short circuit at a certain distance d from the feeding gap, as shown in Fig. 1(a). The short is realized with a metallic interruption of length l_{short} that is assumed to be sufficiently large, so that the magnetic current induced in the slot for $x > d + l_{\text{short}}$ does not influence the current at $x < d$. This assumption allows modeling a semi-infinite slot with infinitely extended metal (for $x > d$) as an infinite slot with a finite metal termination. Such approximation is convenient due to the availability of the infinite slot spectral Green's function in (3). To satisfy the boundary conditions on the metal, an electric current is induced with an edge-singular behavior, as shown in Fig. 1(b). The edge singular basis function is described by:

$$f_g(x) = \frac{2}{g\pi} \frac{\text{rect}_{g/2}(x - (d + g/4))}{\sqrt{1 - \left(\frac{2(x-(d+g/2))}{g}\right)^2}} - \frac{2}{g\pi} \tag{4}$$

The parameter g in (4) is related to the width of the current distribution on the metallic interruption. The value of g was found empirically to be linked to the width of the slot and the free-space wavelength as

$$g = \frac{5}{3}\sqrt{w\lambda}. \tag{5}$$

The average voltage on the delta-gap (v_δ) and on the metallic interruption (v_g), can be expressed as the following system of two linear equations [16]:

$$\begin{cases} v_\delta = i_\delta Z_{\delta\delta} + i_g Z_{\delta g} \\ v_g = i_\delta Z_{g\delta} + i_g Z_{gg} = 0 \end{cases} \tag{6}$$

where i_g is the amplitude of the current on the metallic interruption and we imposed $v_g = 0$ for the perfect conducting termination. The self and mutual impedances are given by

$$Z_{j,i} = \frac{1}{2\pi} \int_{-\infty}^{\infty} \frac{F_i(k_x) F_j(-k_x) e^{jk_x(x_i - x_j)}}{D_s(k_x)} dk_x \tag{7}$$

where the subscripts i and j are either δ or g, $x_\delta = 0$ and $x_g = d$. $F_g(k_x)$ is the spectral expression for the edge singular basis function:

$$F_g(k_x) = e^{jk_x g/2} \times \left(J_0\left(\frac{k_x g}{2}\right) - j\mathbf{H}_0\left(\frac{k_x g}{2}\right) - \frac{2}{\pi}\text{sinc}\left(\frac{k_x g}{2}\right) e^{-jk_x g/4} \right) \tag{8}$$

where $\mathbf{H}_0$ is the zeroth order Struve function.

The input impedance of the slot can now be derived from (6) as the ratio between the average voltage and the current on the delta-gap:

$$Z_{\text{in}} = \frac{v_\delta}{i_\delta} = Z_{\delta\delta} - \frac{Z_{\delta g} Z_{g\delta}}{Z_{gg}}. \tag{9}$$

Figure 2(a) shows the input impedance of a semi-infinite slot in free space calculated as described above, compared to CST. The distance between the excitation gap and the termination of the slot is $d = \lambda_0/4$, the width of the slot is $w = \lambda_0/50$ and the length of the delta-gap is $\delta = \lambda_0/40$, where λ_0 is the wavelength in free space at f_0. Figure 2(b) shows the results of the same slot when a thin dielectric substrate is added. The relative permittivity of the material is $\varepsilon_r = 4$ and the height of the substrate is $h = \lambda_d/20$, where λ_d is the wavelength in the dielectric at f_0. An excellent agreement is shown in both cases.

III. Equivalent Transmission Line Model

The integrand in (7) presents two types of singularities: square-root branch points representing the space waves radiating away from the slot, and poles associated with quasi-TEM waves launched along the slot. When the poles and the branch points coincide, e.g. for a slot on perfectly conducting ground plane radiating in a homogeneous medium, the two

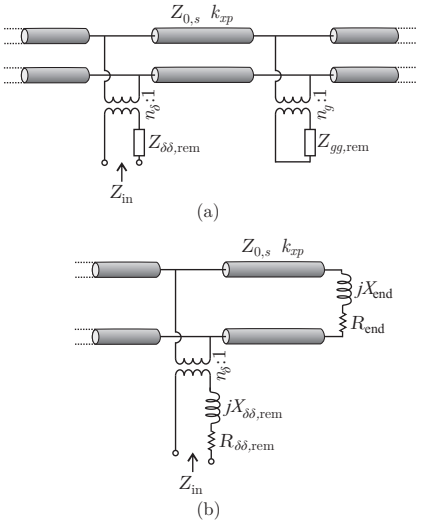

Fig. 3. Equivalent transmission line circuit representing the two basis functions of the semi-infinite slot. (a) The end-point is represented by a transformer and a remaining impedance in parallel to an infinite line. (b) The impedances are represented as resistor accounting for radiation and an inductor accounting for the reactive energy at the feed and the end point.

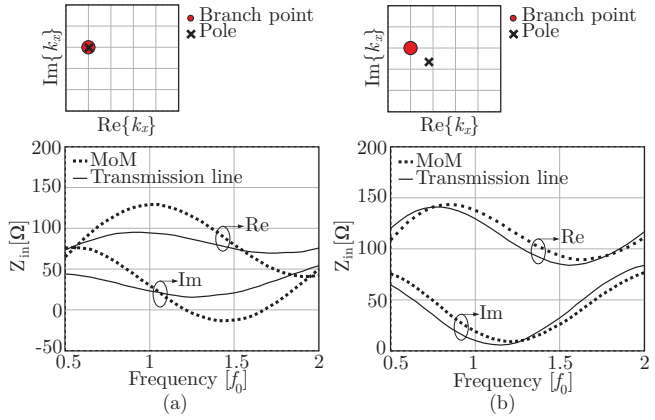

Fig. 4. Comparison between the input impedance of a semi-infinite slot in a lossy ground plane calculated with our method and CST. The geometrical parameters of the structure are $d = \lambda_0/4$, $w = \lambda_0/90$ and $\delta = \lambda_0/90$. λ_0 is the wavelength in free space at f_0. The locations of the pole with respect to the branch point are also shown. (a) $\sigma = 6 \times 10^7\,\mathrm{S\,m^{-1}}$ (b) $\sigma = 1000\,\mathrm{S\,m^{-1}}$.

contributions cannot be considered separately. In these cases the integral in (7) can be solved asymptotically with the method in [14]. This approach allows writing the voltage on the slot for large values of x as the solution of a tapered transmission line with x-dependent characteristic impedance, which is not convenient to model multiple feed points or terminations.

However, introducing losses in the ground plane [12], [15] or a thin dielectric substrate, the pole singularity moves away from the branch point in the complex k_x-plane, so that the polar contribution can be isolated. The location of the pole, k_{xp}, can be found using a local-search algorithm (e.g. Newton's method) starting from k_0. Using Cauchy's theorem the polar contributions to the integrals of (7) in k_{xp} are evaluated. The self impedances are split into their residue contributions and remaining terms $Z_{\delta\delta,\mathrm{rem}}$ and $Z_{gg,\mathrm{rem}}$. For sufficiently large electrical distances d between the feed and the termination, the mutual impedances are well represented by their residual contribution. This allows us to draw an equivalent transmission line circuit representing a semi-infinite slot as shown in Fig. 3(a). For small distances d the interaction between the two basis functions is not described by the mode only propagating along the slot, but also by the space wave coupling, which is not accounted for in the transmission line model.

The turn ratios of the two transformers are equal to $n_\delta = F_\delta(-k_{xp})$ and $n_g = F_g(-k_{xp})$. The characteristic impedance of the transmission line is [12]:

$$Z_{0,s} = -\frac{2j}{D_s'(k_{xp})} \tag{10}$$

where the prime ($'$) indicates the operation of differentiation. The propagation constant along the line is k_{xp}.

We define a single impedance to represent the end-point of the semi-infinite slot:

$$Z_{\mathrm{end}} = \frac{\left(Z_{gg,\mathrm{rem}}/n_g^2\right) Z_{0,s}}{\left(Z_{gg,\mathrm{rem}}/n_g^2\right) + Z_{0,s}}. \tag{11}$$

The two impedances in the circuit are represented explicitly as resistors accounting for radiation and inductors accounting for the reactive energy at the feed and the end point, such that the transmission line circuit is drawn as shown in Fig. 3(b).

Figure 4 shows the comparison between the input impedance of a semi-infinite slot in free space calculated using the previously introduced method of moments and with the transmission line model. The distance between the end-point of the slot and the feeding gap $d = \lambda_0/4$ and the width of the slot is $w = \lambda_0/90$. The length of the feeding gap is $\delta = \lambda_0/90$. Two different surface conductances of the ground plane are considered: $\sigma = 6 \times 10^7\,\mathrm{S\,m^{-1}}$ (copper) and $\sigma = 1000\,\mathrm{S\,m^{-1}}$. The corresponding distances between k_{xp} and k_0 are $(0.0002 - 0.0002j)k_0$ and $(0.086 - 0.0691j)k_0$, respectively, as shown in the figure. It can be seen that for $\sigma = 6 \times 10^7\,\mathrm{S\,m^{-1}}$ the transmission line does not describe the input impedance accurately, as the distance between k_{xp} and k_0 in the complex k_x-plane is too small. In the case when $\sigma = 1000\,\mathrm{S\,m^{-1}}$ this distance is larger and the polar contribution represents better the wave launched along the slot.

Figure 5 shows a similar comparison when a small dielectric is introduced. The dimensions of the structure are the same as in Fig. 2(b). A good agreement is obtained, as the distance between k_{xp} and k_0 is $0.339k_0$ at $f = f_0$. The location of the pole with respect to the branch point is also shown in Fig. 5.

IV. End-Point Impedance

In the previous section an impedance is introduced which describes the end-point of the slot. The impedance is found to be inductive and to have a non-zero resistance, accounting for radiation emerging from the end-point.

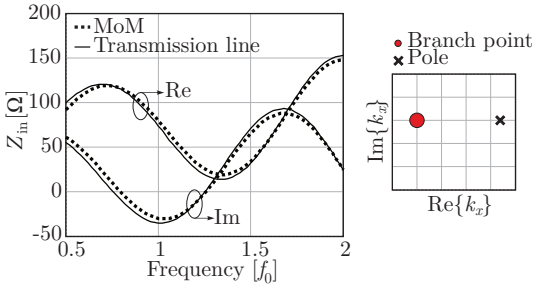

Fig. 5. Comparison between the input impedance of a semi-infinite slot on a dielectric substrate calculated with the transmission line model and the MoM. The geometrical parameters of the structure are $d = \lambda_0/4$, $w = \lambda_0/50$, $\delta = \lambda_0/40$, $h = \lambda_d/20$ and $\varepsilon_r = 4$. λ_0 and λ_d are the wavelengths at f_0 in free space and in the dielectric respectively. The location of the pole with respect to the branch point is also shown.

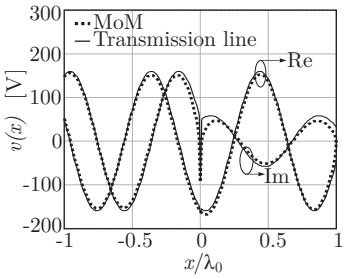

Fig. 6. Comparison between the voltage along a semi-infinite slot on a dielectric substrate calculated with the transmission line model and the MoM. The excitation current is $i_\delta = 1\,\text{A}$. The geometrical parameters of the structure are $d = \lambda_0$, $w = \lambda_0/20$, $\delta = \lambda_0/500$, $h = \lambda_d/20$ and $\varepsilon_r = 4$. λ_0 and λ_d are the wavelengths at f_0 in free space and in the dielectric respectively.

Figure 6 shows the voltage along the semi-infinite slot calculated with the MoM and from the transmission line circuit. Clear differences can be seen around the feeding gap and near the end-point of the slot. The voltage calculated using the transmission line circuit is not zero at the end-point but equal to the voltage across the load Z_{end}. The voltage calculated with the method of moments goes to zero at the end point, but deviates from the sinusoidal distribution close to the termination. This deviation from the sine can be explained by observing the electric field inside the slot. The direction of the electric field inside the slot near the end-point is visualized in CST, and the result is shown in Fig. 7. The electric field along the slot is oriented in the transverse direction, while near the end the field lines bend, in order to be normal to the metal on all three sides. The impact of this bending of the field, and with it the magnetic current, is dependent on the width of the slot. Figure 8 shows the value of Z_{end} for different w. It can be seen that both the inductance and the radiation resistance associated with the end point decrease for narrower slots.

V. Finite Slots

Let us consider the infinite slot on a dielectric substrate, interrupted on both sides of the feeding gap as shown in Fig. 9(a). The edge-singular electric current is induced on both

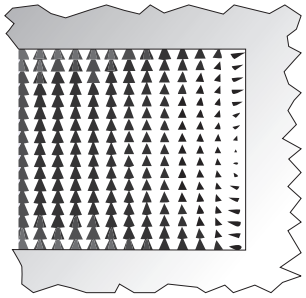

Fig. 7. Electric field lines inside a semi-infinite slot near the end-point.

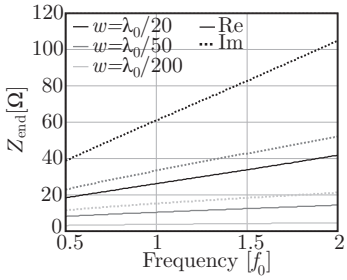

Fig. 8. Values of the end-point impedance Z_{end} as a function of frequency for three different widths of a semi-infinite slot on a dielectric substrate. The height of the substrate is $h = \lambda_d/40$ and $\varepsilon_r = 4$. λ_0 and λ_d are the wavelengths at f_0 in free space and in the dielectric respectively.

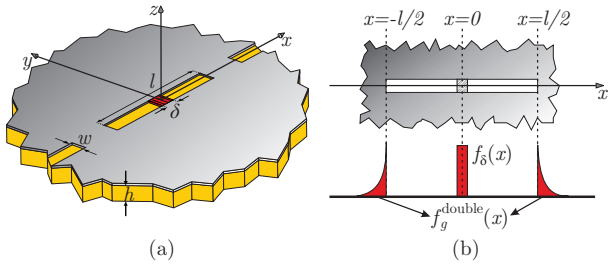

Fig. 9. (a) Infinite slot on a dielectric substrate interrupted on both sides of the feeding gap. (b) Space domain basis functions with respect to their location along the finite slot.

metallic interruptions as shown in Fig. 9(b), such that the boundary conditions are verified.

Since the structure is symmetric, two edge-singular currents on the metal have the same amplitude and the two individual basis functions are combined into one term which is centered around the center of the finite slot:

$$F_g^{\text{double}}(k_x) = F_g(k_x)\, e^{jk_x l/2} + F_g(-k_x)\, e^{-jk_x l/2} \tag{12}$$

where l is the length of the slot. The input impedance of the finite slot can be found, by following the same steps as the semi-infinite slot, to be:

$$Z_{\text{in}} = Z_{\delta\delta} - \frac{Z_{\delta g}^{\text{double}} Z_{g\delta}^{\text{double}}}{Z_{gg}^{\text{double}}}. \tag{13}$$

The transmission line model for the finite slot is very similar to the model of the semi-infinite slotline, but including

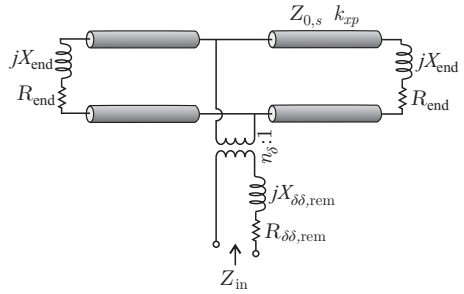

Fig. 10. Equivalent transmission line circuit representing the finite slot in the presence of a thin dielectric substrate.

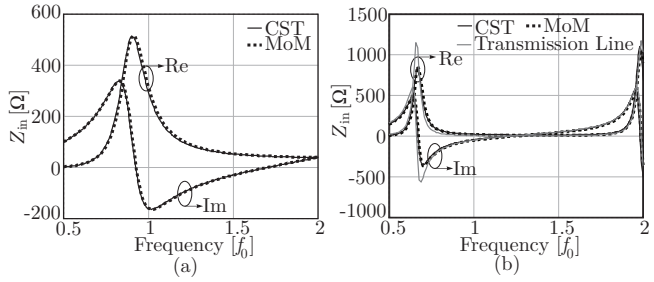

Fig. 11. Comparison between the input impedance of a finite slot calculated with the transmission line model, our MoM and CST. The geometrical parameters of the structure are $l = \lambda_0/2$, $w = \lambda_0/50$ and $\delta = \lambda_0/40$. λ_0 is the wavelength in free space at f_0. (a) The slot is surrounded by free space. (b) A thin dielectric substrate is present: $\varepsilon_r = 4$, $h = \lambda_d/20$ when λ_d is the wavelength in the dielectric at f_0.

terminated transmission lines on both sides, as shown in Fig. 10. Figure 11(a) shows the input impedance of a finite slot in free space calculated with (13), compared to CST. The length of the slot is $l = \lambda_0/2$, the width of the slot is $w = \lambda_0/50$ and the length of the delta-gap is $\delta = \lambda_0/40$, where λ_0 is the wavelength in free space at f_0. Figure 11(b) shows the results of the same slot when a thin dielectric substrate is added. The relative permittivity of the material is $\varepsilon_r = 4$ and the height of the substrate is $h = \lambda_d/20$, where λ_d is the wavelength in the dielectric at f_0. An excellent agreement between the MoM and CST is shown in both cases. The result of the transmission line model is also presented in Fig. 11(b). It can be seen that the accuracy of the transmission line model is better for higher frequency, for which the electrical distance between the feed and the slot ends is larger.

VI. Conclusion

An equivalent transmission line model for planar slots embedded in generic stratified media was presented. The procedure started with deriving an efficient method of moments solution for semi-infinite slots, with only two basis functions, one located at the feeding point and one at the termination of the slot. The basis functions were chosen such that they properly account for the reactive energy localized at these points. The procedure was then extended to a double termination, as to find the input impedance of a finite slot antenna with arbitrary length.

Based on the numerical solution, an equivalent transmission line circuit was derived, by extraction of the pole contribution from the mutual impedance integrals. To be able to separate the residue contribution from the space wave, a thin dielectric slab or losses in the metal can be introduced. The radiation is described in the model as resistances located at the feed and the end points. This approach allows representing the radiation from the slot as the generation of different space waves, one associated with the feeding gap and two emerging from the end points. The physical dimensions and the shape of the basis functions was accounted for in the circuit by means of transformers.

References

[1] C. A. Balanis, *Antenna Theory: Analysis and Design, 4th Ed.* John Wiley & Sons, Inc., Hoboken, New Jersey, 2016.

[2] N. Behdad and K. Sarabandi, "Dual-band reconfigurable antenna with a very wide tunability range," *IEEE Trans. Antennas Propag.*, vol. 54, no. 2, pp. 409-416, Feb. 2006.

[3] C. Occhiuzzi, S. Cippitelli and G. Marrocco, "Modeling, design and experimentation of wearable RFID sensor tag," *IEEE Trans. Antennas Propag.*, vol. 58, no. 8, pp. 2490-2498, Aug. 2010.

[4] Y. Wang and S. Chung, "A short open-end slot antenna with equivalent circuit analysis," *IEEE Trans. Antennas Propag.*, vol. 58, no. 5, pp. 1771-1775, May 2010.

[5] S. B. Cohn, "Slot line on a dielectric substrate," *IEEE Trans. Microw. Theory Tech.*, vol. 17, no. 10, pp. 768-778, Oct. 1969.

[6] R. Garg and K. C. Gupta, "Expressions for wavelength and impedance of a slotline," *IEEE Trans. Microw. Theory Tech.*, vol. 24, no. 8, pp. 532-532, Aug. 1976.

[7] J. J. Lee, "Slotline impedance," *IEEE Trans. Microw. Theory Tech.*, vol. 39, no. 4, pp. 666-672, Apr. 1991

[8] M. Himdi and J. P. Daniel, "Analysis of printed linear slot antenna using lossy transmission line model", *Electronic letters*, vol. 28, no. 6, pp. 598-601, Mar. 1992.

[9] R. Garg, P. Bhartia, I. Bahl, and A. Ittipiboon, *Microstrip Antenna Design Handbook.* Norwood, MA, USA: Artech House, Inc., 2001.

[10] J. E. Ruyle and J. T. Bernhard, "A wideband transmission line model for a slot antenna", *IEEE Trans. Antennas Propag.*, vol. 61, no. 3, pp. 1407-1410, Mar. 2013.

[11] A. Neto and S. Maci, "Green's function for an infinite slot printed between two homogeneous dielectrics. Part I: Magnetic currents," *IEEE Trans. Antennas Propag.*, vol. 51, no. 7, pp. 1572-1581, Jul. 2003.

[12] D. Cavallo, W.H. Syed, and A. Neto, "Equivalent transmission line models for the analysis of edge effects in finite connected and tightly coupled arrays", *IEEE Trans. Antennas Propag.*, vol. 65, no. 4, pp. 1788-1796, Apr. 2017.

[13] S. van Berkel, A. Garufo, N. Llombart, and A. Neto, "A quasi-analytical tool for the characterization of transmission lines at high frequencies," *IEEE Antennas Propag. Mag.*, vol. 58, no. 3, pp. 82-90, Jun. 2016.

[14] D. S. Jones, *Methods in Electromagnetic Wave Propagation, 2nd Ed.* IEEE Press, New York, 1994.

[15] M. Albani, A. Mazzinghi, and A. Freni, "Rigorous MoM Analysis of Finite Conductivity Effects in RLSA Antennas", *IEEE Trans. Antennas Propag.*, vol. 59, no. 11, pp. 4023-4032, Nov. 2011.

[16] D. Cavallo, A. Neto, and G. Gerini, "Analytical description and design of printed dipole arrays for wideband wide-scan applications", *IEEE Trans. Antennas Propag.*, vol. 60, no. 12, pp. 6027-6031, Dec. 2012.